Powder Technology 221 (2012) 351–358

Contents lists available at SciVerse ScienceDirect

Powder Technology

journal homepage: www.elsevier.com/locate/powtec

Electrical conductivity of compacts of graphene, multi-wall carbon nanotubes, carbon black, and graphite powder

Bernardo Marinho [a,b], Marcos Ghislandi [a,d,*], Evgeniy Tkalya [c,d], Cor E. Koning [c], Gijsbertus de With [a]

[a] Laboratory of Materials and Interface Chemistry, Eindhoven University of Technology, 5600 MB Eindhoven, The Netherlands
[b] Department of Chemical Engineering, Federal University of Minas Gerais, Av. Antônio Carlos 6627, 31270-901, Belo Horizonte, Brazil
[c] Laboratory of Polymer Chemistry, Eindhoven University of Technology, 5600 MB Eindhoven, The Netherlands
[d] Dutch Polymer Institute DPI, PO Box 902, 5600 AX Eindhoven, The Netherlands

ARTICLE INFO

Article history:
Received 12 August 2011
Received in revised form 21 December 2011
Accepted 14 January 2012
Available online 21 January 2012

Keywords:
Electrical conductivity
MWCNTs
Graphene
Polymeric composites

ABSTRACT

The electrical conductivity of different carbon materials (multi-walled carbon nanotubes, graphene, carbon black and graphite), widely used as fillers in polymeric matrices, was studied using compacts produced by a paper preparation process and by powder compression. Powder pressing assays show that the bulk conductivity depends not only on the intrinsic material properties but is also strongly affected by the number of particle contacts and the packing density. Conductivities at high pressure (5 MPa) for the graphene, nanotube and carbon black show lower values (~10^2 S/m) as compared to graphite (~10^3 S/m). For nanotube, graphene and graphite particles, the conductive behavior during compaction is governed by mechanical particle arrangement/deformation mechanisms while for carbon black this behavior is mainly governed by the increasing particle contact area. The materials resulting from the paper preparation process for carbon black and graphite showed similar conductivity values as for the compacts, indicating a limited effect of the surfactant on the conductivity. The paper preparation process for the large surface area nanotube and graphene particles induces a highly preferred in-plane orientation, thereby yielding largely the single particle intrinsic conductivity for the in-plane direction, with values in the order of 10^3 S/m.

1. Introduction

The discovery of graphitic nanoparticles with exceptional electrical transport properties, like high conductivity and high charge mobility, has incredibly broadened the range of potential applications of this class of materials, thus unleashing a revolution in the electronic device industry. Two of the most important members of this new generation of materials are undoubtedly carbon nanotubes and graphene [1–6].

Particularly in composite science and technology, current studies have shown that the incorporation of these two materials into polymeric matrices is capable of enhancing the electrical conductivity of polymers by several orders of magnitude without compromising other important features, such as the mechanical and optical properties [7,8].

Perhaps the biggest challenge to be faced at this stage is how to manipulate these nanoparticles in order to bring effectively their remarkable electrical properties onto the macroscopic level. Since the conductivity of a composite is directly related to the formation of a conductive network through the polymer matrix [9,10], its understanding depends, at least partly, on the knowledge of the electrical behavior of the nanoparticles agglomerates, here called bulk powder.

Traditionally, due to its simplicity and reproducibility for many systems, the electrical behavior of both metallic and non-metallic powders [11–16] is characterized by monitoring the electrical conductivity of these powders under compression. This method has also been employed recently to study the electrical resistivity of carbon microtube compacts as a function of filament diameter and graphitization technique [17].

Recent studies with filtered dispersions of carbon nanotubes produced highly oriented films in which some of the favorable intrinsic features of these nanomaterials, such as their electronic and thermal transport properties, are duly reflected. These films, known as buckypapers, consist of paper-like structures in which the nanoparticles are joined together by van der Waals interactions and present promising materials for investigating their properties macroscopically, not only for the nanotubes [18] but also for graphene [19]. Similar structures can be made from other carbon fillers and we refer to these generically as papers or if a specific carbon filler such as graphene is used as graphene paper.

The electrical conductivity of a bulk powder is generally lower than that of the individual particles, since the interface between the particles offers extra resistance to charge transport. The application of pressure increases the conductivity basically by enlarging the

* Corresponding author at: Laboratory of Polymer Chemistry, Eindhoven University of Technology, 5600 MB Eindhoven, The Netherlands. Tel./fax: +31 40 2473066/2445619.
E-mail address: M.G.Ghislandi@tue.nl (M. Ghislandi).

0032-5910/$ – see front matter © 2012 Elsevier B.V. All rights reserved.
doi:10.1016/j.powtec.2012.01.024

contact area between the particles; some elastic and plastic deformation also may happen. In the final stage, which corresponds to the theoretical maximum degree of compaction (i.e. in principle 100% relative density), single particle conductivity is generally not reached, since the contact effects cannot be completely eliminated [20,21].

In this work, four different carbon fillers have been studied: multi-walled carbon nanotubes (MWCNTs), graphene, graphite and carbon black (CB). Except for CB, which consist of a mixture of sp^2- and sp^3-hybridized carbon atoms, all other materials are mainly formed from a sp^2 honeycomb network. Interpreting the conductivity of these materials is a challenging task. In literature [2–7] their intrinsic conductivity is studied. In this article the powder (bulk) and paper conductivity are measured, related to structure and intrinsic conductivity and their relevance in the field of composites processing technology discussed.

2. Experimental

In order to study the electrical conductivity of carbon-based materials, two different processing conditions were applied. The first one consists of monitoring the electrical conductivity during the compaction of powders, whereas the second involves the preparation of paper films and measuring their conductivity. The conductivities of both compact and paper were studied as a function of the bulk density, defined by $\rho = m/Al$, where m is the mass of material, A is the area and l is the thickness of the specimens.

2.1. Materials

Purified long thin MWCNTs (*Nanocyl® 7000*, Nanocyl Belgium) were used. The tubes were produced according to the "Catalytic Carbon Vapor Deposition" method; carbon purity 90%. Graphene sheets (*SP-2 Bay Carbon*) used were obtained via graphite oxidation and a thermo-expansion process [22]. XPS shows an amount of oxygen content around 15% while TEM studies indicate at least 50% of single sheets.

Electroconductive CB (*Ketjenblack® EC-600JD*, AkzoNobel) and synthetic graphite (*SP-2 Bay Carbon*, mesh size below 200), whose compaction behavior has already been extensively documented in literature [11–16], were used for the sake of comparison and also to verify the reliability of the pressing device measurements. SEM and TEM characteristics are shown in Fig. 1.

Nitrogen adsorption analysis (Micromeritics TriStar 3000) was employed for further morphological characterization of the powders. The samples were degassed for 12 h at 150 °C in vacuum. The surface area was calculated in accordance with the BET method [23].

2.2. Paper preparation

The filler dispersions were prepared with the surfactant polystyrene sodium sulfonate (PSS, Aldrich, $M_w = 70.000$ g/mol). Initially, 0.08 g of filler was added to an 80 ml (100 ml flask) aqueous solution containing surfactant (PSS, ratio PSS/H_20 equal to 1/1). The dispersion was made via a sonication process, promoted by a horn sonicator (Sonic Vibracell VC750) with a cylindrical tip (10 mm end cap diameter) for 2 h. The output power was set as 20 W. For the purpose of controlling the temperature, the container with the mixture was immersed in a bath of ice during the sonication process. The quality of the dispersion was verified by monitoring the process via UV–Vis spectroscopy [24].

10 ml of the filler dispersion, prepared according to the previous procedure, was transferred into a filtration set up containing a polyamide membrane with a pore size of 0.45 μm and then pressurized.

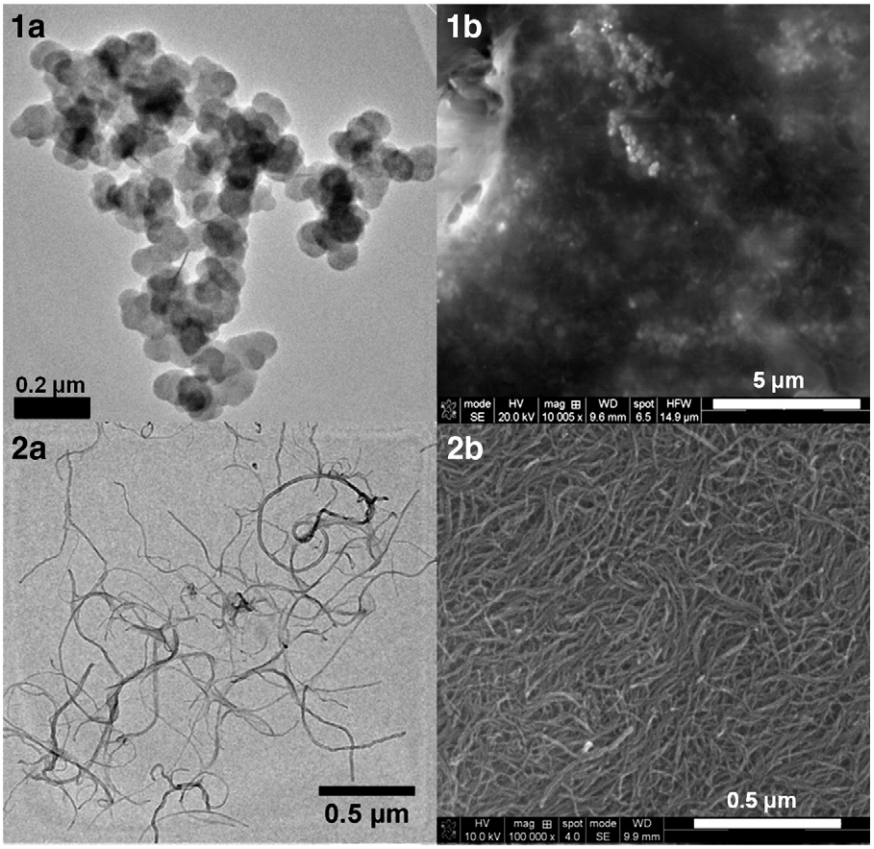

Fig. 1. TEM images (left side) reveal the grape-like aggregation of CB spheres (1a) and a few multi-walled carbon nanotubes (2a). SEM images (right side) show the packing of CB inn the paper-like structures (1b) and the boiled spaghetti organization of the tubes oriented in the surface direction (2b).

As a result of the filler sedimentation, a smooth and black film was formed on the filter surface. In order to remove residual moisture, the films were dried at 90 °C under 200–400 mbar in a vacuum oven for 3 h.

The dc electrical resistance of the papers (and also of the powder compacts) for the in-plane (longitudinal) direction was measured via the four-point method. The electrical current was provided by a source-measure unit (Keithley 237), while the voltage was measured by an electrometer (Keithley 6517A). It should be emphasized that for each sample several values of the current were tested until the ohmic range was established. For each value, six values of applied current I and their correspondent voltages V were registered and the resistance R was calculated from Ohm's law, i.e. from $R=V/I$. The electrical contact between the sample and the equipment was done via four indented copper pins (3 cm length) pressed against four 1 cm long parallel silver paste lines painted on the surface of the paper, with an internal interval length l of 0.5 cm. The cross-section area A was obtained by multiplying the 1 cm long lines (corresponding to the width) with the thickness of the samples. The conductivity σ was then estimated according to $\sigma=l/AR$. For the measurements on the transversal direction the papers were cut (Ø 1.19 cm) and measured with the powder pressing setup according to procedure described in Section 2.3.

2.3. Powder pressing

The compression assays were performed in especially designed equipment, based on the information in [15], and schematically shown in Fig. 2. The device consists of a thick isolating ceramic die (inner diameter 1.20 cm), vertically fixed on a heavy circular copper support containing a stationary piston (1.19 cm thick, 1 cm length) that closes the bottom of the cylinder. A close-fitting copper plunger (1.19 cm thick, 4 cm length), which is allowed to move down in the cylinder, closes the compression chamber. After filling the chamber with an accurately weighed amount of powder, the load applied on the piston was controlled by a universal testing machine (Lloyd EZ20), varying from 5 to 500 N, which resulted in a pressure range from 50 kPa to 5 MPa. Such a range, although apparently wide, proved to provide good electric contacts in the particle bed without damaging its structure [15].

The dc electrical resistance of the compressed powders (and also of the papers on the transversal direction) was measured via the four-point method. The electrical current was provided by a source-measure unit (Keithley 237), while the voltage was measured by an electrometer (Keithley 6517A). For each pressure, five values of the applied current and the corresponding voltages were registered and the resistance was calculated. The conductivity was then estimated according to $\sigma=l/AR$, where l represents the powder column height, obtained by the displacement of the piston and A is the cross-section area of the piston.

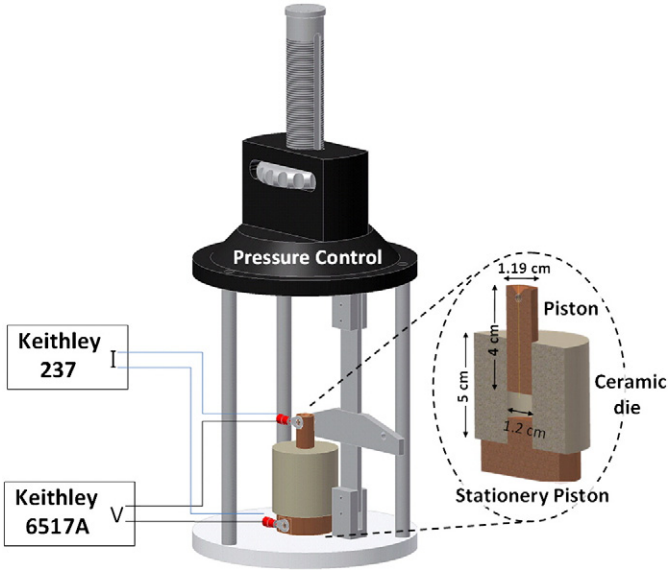

Fig. 2. Schematic representation of the experimental setup involved in the measurement of the powder density and conductivity.

The electrical contact between the sample and the copper pistons was enhanced by polishing the two surfaces area of the metal exposed to the filler (1.13 cm^2) and direct pressing against the weighted amount of powder. No silver paint was necessary. The electrical resistivity of the apparatus itself (copper pistons in contact with each other plus cable contacts tightly screwed to the pistons) was verified and found to be lower than $10^{-6}\,\Omega\cdot m$, consequently not compromising the powder measurements. This measurement was done via four point method with the absence of powder; varying the pressure from 50 kPa to 5 MPa, with no change in resistance observed.

3. Results and discussion

3.1. Amount of powder for pressing

The amount of powder used to fill the die plays an essential role in the success of a compression experiment. Indeed a certain minimum number of particles are required in order to achieve representative results. Moreover, small amounts of material are more susceptible to edge effects like particle orientation, since the proportion of material in contact with the piston and chamber walls is relatively high. On the other hand, a too large amount of material causes a less homogeneous pressure distribution, which unavoidably leads to density gradients, directly affecting the reliability of the experiment [15]. Therefore, it is indispensible to determine a proper range of mass for each material before interpretation of the acquired data can be done reliably. Hence, preliminary pressing essays with different amounts of powder were performed and compared.

For small quantities of powder, the conductivity is extremely variable, suggesting that the previously discussed low-amount effects are present. From a certain value of the initial powder column height, though, the conductivity during compaction is no longer strongly dependent on the amount of material for every pressure, which means that the "homogeneity" conditions are met. In a certain range after this point, the conductivity measured proved to be insensitive to the amount of powder used. Hence a column height range where the conductivity value is stable was used in the measurements. This is value is higher for graphite and CB (more than 6 mm) than for MWCNTs and graphene (about 3 mm), suggesting that for graphite and CB a smaller number of contacts is present as compared to MWCNTs and graphene. Based on this, the amount of powder material and initial column height selected for analyses were respectively: graphite, 0.75 g ± 0.001 and 9.9 mm ± 0.1; CB, 0.5 g ± 0.001 and 12.6 mm ± 0.1; MWCNTs 0.1 g ± 0.001 and 13.4 mm ± 0.1; Graphene, 0.1 g ± 0.001 and 16.8 mm ± 0.1.

3.2. Density versus pressure

Fig. 3 shows the density as a function of pressure (ρ–P curve). The data shown are the average of three measurements, the results of which differ by no more than 3%.

As can be seen, the different fillers show similar densification–pressure behavior, namely a bi-linear dependence on the logarithmic pressure, as has been often noticed in the ceramic literature, a particularly clear reference being [25]. This behavior is interpreted as follows. The morphology of the carbon powders consists of agglomerates, built up from many primary particles. After filling the die, a loosely

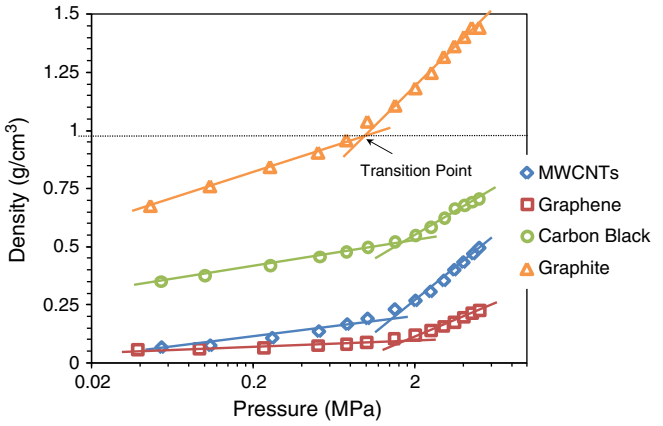

Fig. 3. Density as a function of pressure (ρ–P curve) for the various powder compacts. Data given are the average of 3 experiments with values varying less than 3%.

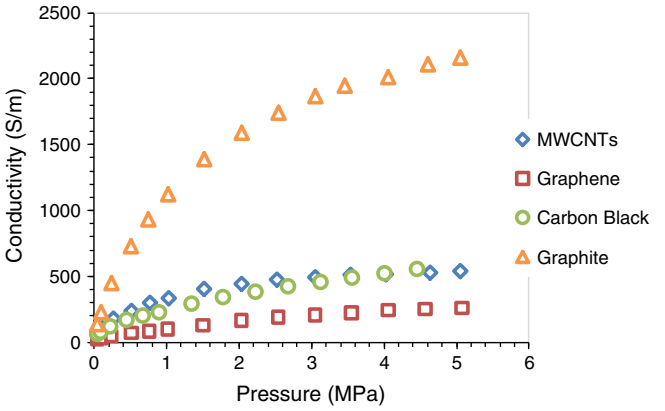

Fig. 4. Electrical conductivity behavior of the different carbon powders as a function of pressure. For each material the data points represent an average of at least 3 identical assays differing not more than 3%.

packed compact results with large voids between the agglomerates. In the low pressure region, densification is due mainly to rearrangement and fragmentation of relatively weak agglomerates controlled by particle–particle friction; no significant change in internal agglomerate structure is expected. This behavior is represented by the first linear portion of each curve in Fig. 3. At pressures exceeding a transition point, however, densification mainly is a result of compression (elastic/plastic deformation) of the agglomerates; the process is controlled by forces between the primary particles within the agglomerates. Densification will increase as a result of rearrangement and reduction of intra-agglomerate primary-particle distances (second linear portion of curves in Fig. 3).

One of the few simple approaches, if not the only one, that takes these two processes explicitly in to account is due to Cooper and Eaton [26]. According to these authors the large pore distribution between the agglomerates and the small pore distribution between the particles within the agglomerate can be described by the dependence of the normalized volume fraction $V^* = (V_0 - V)/(V_0 - V_\infty)$ on pressure P, where V represents the actual volume and V_0 and V_∞ the initial and final volume, respectively. This relation reads

$$V^* = V_l^* + V_s^* = a_l e^{-b_l/P} + a_s e^{-b_s/P} \quad (1)$$

where a_l (a_s) and b_l (b_s) are constants related to large (small) pore contribution. Eq. (1) was used to fit the experimental data for the different carbon fillers and results are shown in Table 1.

Overall the values for the RMSDs indicate an excellent fit with a maximum difference less than 5% and an average difference of about 1%. According to the Cooper-Eaton approach $a_l + a_s$ should equal 1, a condition reasonably well fulfilled for all materials (see Table 1). Finally we note that the transition points, as indicated in Table 3, corresponds with the pressure P_t where $dV_l^*/dP = dV_s^*/dP$ holds. For MWCNTs, for instance, $P_t \cong 1.5$ MPa.

3.3. Conductivity versus pressure

Conductivity versus pressure data are shown in Fig. 4. The data represent an average of three measurements, the results of which differ not more than 3%, indicating good reproducibility. A comparison of powder and paper conductivity is given in Table 2, together with data on specific surface area and intrinsic conductivity.

Surprisingly, the highly conductive single particles such as MWCNTs and graphene, when pressed together, exhibit lower conductivity values than graphite (see Table 2). Also the two processing methods, powder pressing and paper, do generate different conductivity values (see Table 2).

Clearly the constriction of the current flow due to contact spots plays a major role when comparing the bulk conductivity of different powders. As expected, for none of the carbon materials the single particle conductivity was reached by the bulk materials, due to the impossibility of annulling the contact resistance effect. Interestingly, the conductivity of a single particle of carbon black differs by only a factor of 2, as compared with the conductivity obtained by powder pressing.

CB as used in this work can be considered as spherical agglomerates and hence the same kind of contacts in both powder and paper are expected. Indeed the CB paper conductivity only shows a slightly lower conductivity value as compared to the powder pressed at the same density. A similar remark can be made for graphite, although here the difference is somewhat larger. Since the density is the same, this small decrease is probably caused by the remaining amount of surfactant. For nanotubes and graphene this difference reaches up 5 and 6 orders of magnitude, respectively. This indicates that the contact resistance influence is far more pronounced for the nanoparticles (MWCNTs, graphene) than for the microparticles (graphite, carbon black) structures.

An increasing conductivity with increasing particle diameter has also been observed for carbon filaments [17] and has been attributed, among other reasons, to the decreasing effect of contact resistance

Table 1
Fit parameters for volume fraction calculation.

Filler	a_l	b_l	a_s	b_l	RMSD
MWCNTs	0.749	0.130	0.275	1.537	0.012
Graphene	0.337	0.113	0.788	1.785	0.011
Carbon black	0.440	0.089	0.465	2.845	0.010
Graphite	0.513	0.070	0.485	1.606	0.006

Table 2
Material and compact characteristics.

Filler	BET surface area (m^2/g)	Conductivity (S/m)			
		Powder compact at 5 MPa	Paper	Isolated Single particle conductivity	Filler contribution limit from compact[a]
MWCNTs	272	5.43×10^2	5×10^3	10^6–10^{7}[b]	10.3×10^3
Graphene	180	2.62×10^2	1.4×10^3	10^7–10^8 [2]	10.9×10^3
Carbon Black	56.9	5.58×10^2	9×10^1	10^3 [14]	8.8×10^3
Graphite	3.08	2.12×10^3	1.2×10^3	10^5 [27][c]	13.8×10^3

[a] Estimate based on the model as described in [17].
[b] As provided by the Nanocyl Company: http://www.nanocyl.com/en/CNT-Expertise-Centre/Carbon-Nanotubes.
[c] Value highly variable depending on source.

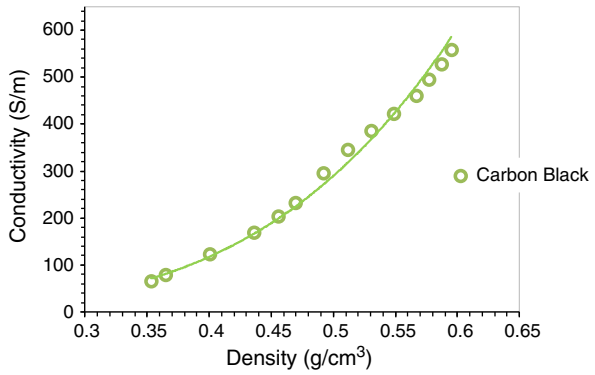

Fig. 5. Conductivity σ of CB as a function of density ρ. The line represents the fit with $\sigma \approx \rho^4$ using the Kendall approach.

with increasing particle size. Due to the much higher surface area of the nanoparticles, as confirmed by BET, the number of contacts is much higher as compared to the microparticles for the same amount of material in the same volume. Table 2 also shows a simple calculation for the expected conductivity of the fillers in the compact utilizing a model described in literature [17] based on the rule of mixtures and assuming a random geometric configuration of the fillers during compaction in 3D space. The contribution of filler conductivity σ_f in a compact is represented by $\sigma_f = 3\pi\sigma/2V_f^*$, where $3\pi/2$ is the geometric factor, σ is the powder compact conductivity at pressure of 5 MPa and V_f^* the volume fraction of fillers at the same pressure. This equation represents the expected conductivity of the particles in the compacts assuming no contact resistance, and was used to estimate the high conductivity limits of carbon filaments from compacts. It provides a good indication of the achievable conductivity for the fillers, taking into account the different density states they present.

The conductivity and specific surface area do not show a straight forward relation, as others parameters like particle shape, interfacial forces between particles, electron transport mechanism and packing density, are also factors that influence the bulk conductivity. For the nanoparticles, although the paper density was not achieved for the powder compacts, the huge discrepancies as observed between the powder and the paper values suggest some preferred particle orientation, probably caused by their anisometric shape, as discussed in Section 3.5.

3.4. Conductivity versus density

Some further information can be extracted from the conductivity versus density behavior. We discuss first the results for CB and thereafter the other results. The variation of the conductivity σ of CB with the density is displayed in Fig. 5.

Due to its grape-like structure, packing of CB is often considered as an isotropic packing of spheres. Conductivity depends on the contact diameter between grains, and this can be calculated from the van der Waals attractive forces, knowing the size and elastic modulus of the particles [14,28]. There is also a strong dependence on particle volume fraction ϕ and this has been modeled by a ϕ^4 relation [29], resulting from a generalization of equations as derived for equal-sized spheres packed in various lattice types [30]. This reasoning led to [14]

$$\sigma = 40.6\sigma_*\phi^4\left[\frac{\Gamma\left(1-\nu^2\right)}{ED}\right]^{1/3} \quad (2)$$

for the electrical conductivity σ with D the particle diameter, E Young's modulus, ν Poisson's ratio, σ^* the single particle conductivity, 40.6 a constant related to packing, and Γ the interface energy of the contact surface between the particles. This equation was successfully used to fit conductivity versus density for CB [14] as well as Ti_4O_7, TiN and TiB_2 [28] powders.

Regression of experimental data according to Eq. (2) results in $\sigma = 4768\rho^{4.0}$, with a correlation coefficient of 0.995. From the fit results using the reference values for CB $E = 24$ GPa [14], $\nu = 0.3$, $\sigma^* = 4000$ S/m [14], $\rho^* = 0.80$ g/cm^3 [15] and estimating $D = 100$ nm from SEM images (Fig. 1), the interface energy was found to be 4.6 mJ/m^2. This value is in reasonable agreement with the 6 mJ/m^2 obtained by Kendall [14], taking into account that the results are sensitive to small changes in conductivity and density and are carried out in different equipments and probably using different CB powders [12,15].

Note that the particle size as estimated from the specific surface area, 0.13 μm, differs slightly from the SEM estimate, 100 nm. This is probably due to the experimental uncertainty for the SEM measurements due to the limited number of particles analyzed.

Also note that for CB there is no clear transition point in the ρ–σ curve, like it was observed for the ρ–P curve. This indicates that the conductive behavior is not directly influenced by the mechanisms controlling compaction, i.e. initial re-arrangement/fragmentation followed by elastic/plastic deformation of the agglomerates. Good conductive contacts are established in the initial low density regime even before deformation. This might be related to local plastic deformation at the contact points long before overall plastic deformation takes place, as shown by the ρ–P curve.

For the other materials, a plot of conductance G versus density ρ suggests a bi-linear relationship (Fig. 6). For these materials with anisometric particles one can clearly indentify a transition point (Table 3), as described before, being interpreted as agglomerate rearrangement/fragmentation for the low density, and elastic/plastic deformation for

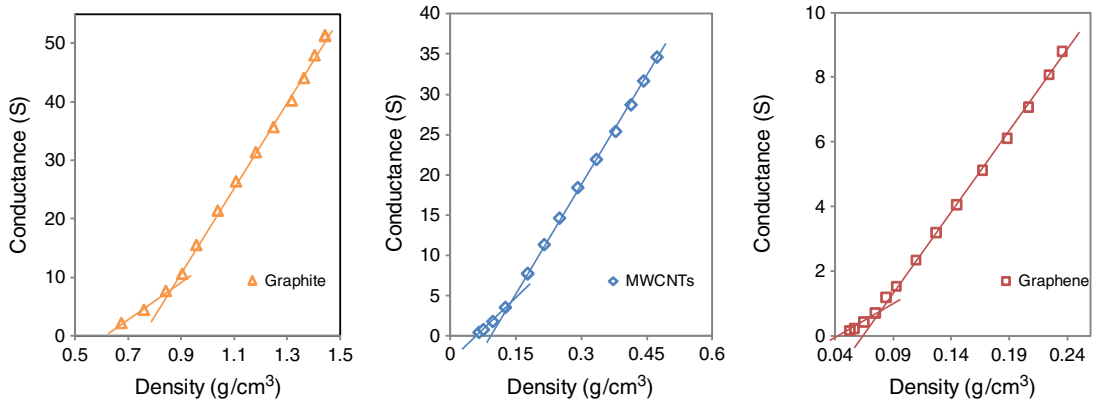

Fig. 6. Conductance of the various powders as a function of density.

Table 3
Density transition points according to mechanical and electrical characterization.

Filler	Density transition points(g/cm^3)		Fit parameters for the Holm equation		
	ρ–P curve (Fig. 3)	G–ρ curve (Fig. 6)	α	β	RMSD
Graphite	0.97	0.87	1182.4	0.38	43.47
MWCNTs	0.19	0.14	348.6	0.29	15.43
Graphene	0.10	0.08	108.5	0.57	6.62

Table 4
Thickness, average in-plane and transverse conductivities for powder compacts and papers of MWCNTs and graphene.

Filler	Type	t (mm)	$\sigma_{\parallel}$ (S/m)	$\sigma_{\perp}$ (S/m)
MWCNTs	Compact	1.32	3.4×10^{2}	5×10^{2}
	Paper	0.045	5×10^{3}	1.4×10^{-2}
Graphene	Compact	1.10	1.3×10^{2}	2.7×10^{2}
	Paper	0.03	1.4×10^{3}	1.6×10^{-1}

the high density part. These two mechanisms have a direct influence on the conductance behavior of these particles.

An interesting point observed for all three materials is a small shift of the transition points to lower density values, when we compare values extracted from the ρ–P curve (Fig. 3) and values extracted from the ρ–G curve (Fig. 6), respectively (Table 3). This shift indicates that good contact or a higher number of electrical contacts starts to form a bit before the starting of the deformation/fracture regime. The assumption that good contact can be established already during rearrangement can rationalize this shift.

Holm [31] proposed a relation between conductivity σ and pressure P based on an increasing contact area between particles upon increasing the pressure, which reads:

$$\sigma = \alpha P^{\beta} \tag{3}$$

with α and β constants. The value for β is predicted to be 0.5 for elastic contact and 0.33 for plastic contact. This equation was used to fit the experimental data shown in Fig. 4 above the transition point and the results are also given in Table 3. The low values for the RMSDs (maximum difference below 10% and average difference below 1%) indicate the good fits. While the β-value for graphene is close to 0.5, the β-values for graphite and MWCNTs are closer to 0.33, indicating the difference in deformation behavior. Interestingly, the behavior of the CB could also be fitted well with the Holm equation. The β-value of about 0.5 indicates primarily elastic contact, in agreement with the Kendall model.

3.5. Orientation dependence

In order to detect preferred particle orientation, the conductivity of both the powder compacts and papers were measured for the surface (in-plane) direction and also for the transverse (through-the-sample) direction (see Fig. 7). The in-plane conductivity was measured following the procedure described in Section 3.2 and the transverse one directly in the pressing device. The compacts of MWCNTs and graphene result from pressing these powders into tablets at 5 MPa during 2 h. Three samples of each material were produced, with a variation in conductivity lower than 3% for the transverse direction and lower than 10% for the in-plane direction. The papers of MWCNTs and graphene were prepared according to the procedure described in Section 3.2 after which the filter membrane was removed. Three samples (10 mg each) were prepared from each material, with a variation of less than 10% in conductivity for the in-plane measurement direction and less than 5% for the transverse one.

The results obtained are shown in Table 4. The in-plane ($\sigma_{\parallel}$) and transverse ($\sigma_{\perp}$) conductivities are similar for the powder compacts, whereas for the papers a huge difference (four to five orders of magnitude) in conductivity was observed. The average areal density was found 0.0024 g/cm^2 for graphene paper and 0.0027 g/cm^2 for MWCTs paper; the average thickness t is shown in Table 4.

Even high mechanical loading was not able to alter significantly the random character of the particle arrangements in the powder compacts. It was thus assumed that the carbon nanotubes still find themselves entangled in a “boiled spaghetti-like” structure, and that graphene sheets, besides disoriented, are mostly folded. On the other hand, the huge difference between the conductivity for the in-plane and transverse directions for the papers suggests that a high in-plane orientation of the particles is achieved during paper formation. Dispersion plus sonication promotes the exfoliation to individual particles, which are initially aggregated in bundles, and therefore the alignment of the nanotubes and the unfolding of the graphene sheets. The slow process of vacuum filtration gives the individual particles time to sediment and organize, forming a well-oriented film. This was also visualized by SEM analyses of the graphene fillers, as shown in Fig. 8.

Note though, that since the papers are around 300 times thinner than their corresponding compacts, direct comparison is not straightforward. Apart from the relative ease of sedimentation/organization for the papers, a thicker sample usually contains less orientated particles since displacement/reorientation of particles during compaction is more hampered. Finally, in spite of the consistent conductivity–pressure behavior as observed for the compacts, density gradients may play a role.

It was already noted that the influence of the surfactant, adsorbed on the filler and possibly hampering electronic transport, was negligible for compacts of the spherical CB particles. It is impossible to produce proper papers without the use of surfactants, as they are

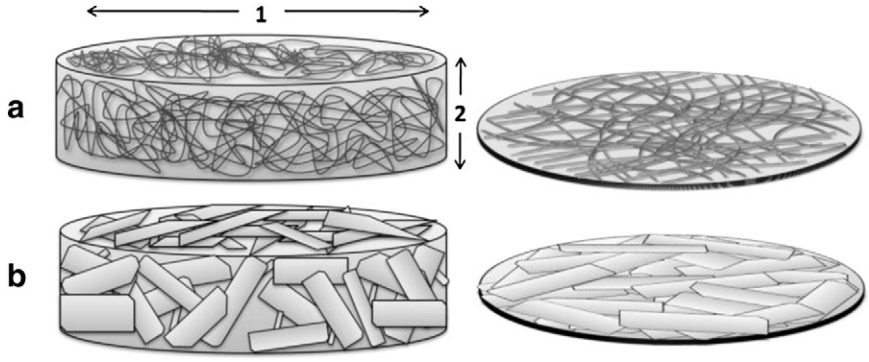

Fig. 7. Carbon nanotubes (A) and graphene sheets (B) organized into compacts (left) and papers (right). Conductivity was measured for the in-plane (1) and transverse (2) directions.

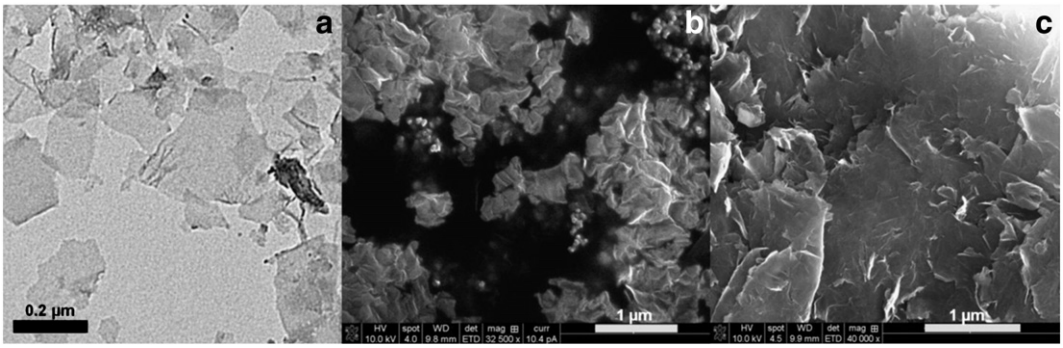

Fig. 8. TEM image of isolated folded and unfolded graphene sheets after exfoliation/dispersion (8a), SEM image showing the highly entangled structure of wrapped graphene platelets, as observed in both powder and compacts (8b), and SEM surface image of in-plane oriented graphene platelets in paper-like structures (8c).

required to realize stable dispersions in water and proper filtering in order to obtain homogeneous paper films. Alternatively, we measured the conductivity during powder compaction using a powder with the same surfactant/filler ratio as used for the paper preparation and compared the results with results obtained for pure MWCNTs. The curves, shown in Fig. 9, confirm that a difference of around 25% at higher pressures, which is negligible as compared to the orders of magnitude difference observed for the other systems studied.

4. Conclusions

We studied four forms of carbonaceous materials: MWCNTs, graphene, graphite and CB. The differences in their electrical behavior, as observed using powder compaction and paper formation, reflect their distinct morphologies.

With powder compaction for all the materials, the bulk conductivity depends basically on the packing density. In a first pressing stage, the density is controlled by rearrangement and fragmentation of agglomerates, followed by a second regime where the elastic and plastic deformation determines the density. The conductive behavior is directly governed by these two mechanisms for the materials with anisometric particles, i.e. graphite, MWCNTs and graphene. For carbon black the relation is not straight forward and good conductive contacts are already formed at relative low density, below 0.5 g/cm^3, before overall deformation.

In the case of MWCNTs and graphene, on top of the packing density influence described above, the orientation of the fillers proved to influence the bulk conductivity behavior significantly. For these materials, which consist of anisometric nanoparticles with high surface area, powder pressing conductivity curves showed unexpected low values, almost ten times lower as compared to graphite, probably due to the high number of particle contacts, which diminish the overall bulk conductivity measured on a macroscopic scale. On the other hand, papers produced with these materials largely preserved their intrinsic conductive properties for the in-plane direction, reaching a maximum of around 5×10^3 S/m for the MWCNTs. This processing method is therefore useful for the sake of comparison when developing new synthesis routes for carbon-based composites. Comparison of results for powder compacts with and without using surfactant, necessary to obtain good papers, showed that the influence of the surfactant on the conductivity is negligible.

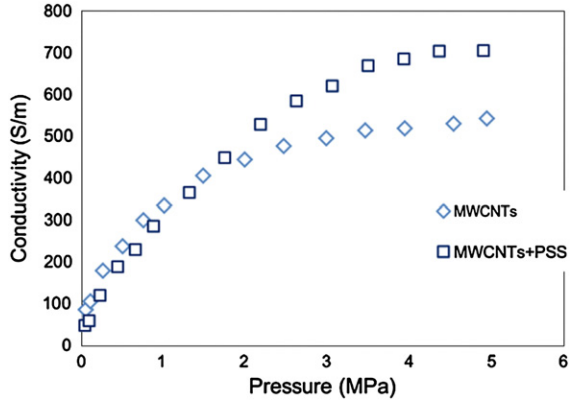

Fig. 9. Electrical conductivity behavior of MWCNTs powders, with and without surfactant present, as a function of pressure. For each material the data points represent an average of at least 3 identical assays differing not more than 3%.

The fact that (relatively) high bulk conductivity can be reached with (relatively) low intrinsic conductivity materials using random structures as in powder compacts, indicates that optimal processing is of the utmost importance. The successful fitting achieved for powder pressing assays shows that this method can clarify the influence of different compaction mechanisms on the final conductivity. Its high reproducibility, in addition to its simplicity and low cost, make powder pressing suitable for processing control of filler production.

Acknowledgments

This work forms part of the research program of the Dutch Polymer Institute (DPI), project number 648. We would like to acknowledge Dr. Kangbo Lu for the TEM images, Huub van de Palen for helping with the powder pressing set up development and Dr. Adolphe Foyet for the support with the conductivity measurements.

References

[1] E. Gogotsi, Nanomaterials Handbook, CRC Press, 2006.
[2] J. Chen, C. Jang, S. Xiao, M. Ishigami, M.S. Fuhre, Electronic properties and devices: intrinsic and extrinsic performance limits of graphene devices on SiO_2, Nature Nanotechnology 3 (2008) 206–209.
[3] A.K. Geim, Graphene: status and prospects, Science 324 (2009) 1530–1534.
[4] C. Li, E.T. Thostenson, T. Chou, Sensors and actuators based on carbon nanotubes and their composites: a review, Composites Science and Technology 68 (6) (2008) 1227–1249.
[5] K.S. Novoselov, A.K. Geim, S.V. Morozov, D. Jiang, Y. Zhang, S.V. Dubonos, et al., Electric field effect in atomically thin carbon films, Science 306 (2004) 666–669.
[6] S. Ijima, Helical microtubules of graphitic carbon, Nature 354 (1991) 56–58.
[7] M. Moniruzzaman, K. Winey, Polymer composites containing carbon nanotubes, Macromolecules 39 (2006) 5194–5205.
[8] S. Stankovich, D.A. Dikin, G.H.B. Dommett, K.M. Kohlhaas, E.J. Zimney, E.A. Stach, et al., Graphene-based composite materials, Nature 442 (2006) 282–286.
[9] E. Tkalya, M. Ghislandi, A. Alekseev, C. Koning, J. Loos, Latex-based concept for the preparation of graphene-based polymer composites, Journal of Materials Chemistry 20 (2010) 3035–3039.
[10] J. Yu, K. Lu, E. Sourty, N. Grossiord, C. Koning, J. Loos, Characterization of conductive multiwall nanotube/polystyrene composites prepared by latex technology, Carbon 45 (2007) 2897–2903.
[11] T. Noda, H. Kato, T. Takasu, A. Okura, M. Inagaki, The electrical resistivity of carbon black under compression, Bulletin of the Chemical Society of Japan 39 (1966) 829–833.
[12] K.J. Euler, R. Kirchhof, H. Metzendorf, The electric conductivity and related phenomena of compressed powder materials, Materials Chemistry 4 (4) (1979) 611–629.

[13] A. Espinola, M. Mourente, M. Salles, A. Pinto, Electrical properties of carbons—resistance of powder materials, Carbon 24 (1986) 337–341.
[14] K. Kendall, Solid surface energy measured electrically, Journal of Physics D: Applied Physics 23 (1990) 1329–1331.
[15] A. Celzard, J.F. Marêche, F. Payot, G. Furdin, Electrical conductivity of carbonaceous powders, Carbon 40 (2002) 2801–2815.
[16] X. Shui, D.D.L. Chung, Submicron diameter nickel filaments and their polymer-matrix composites, Journal of Materials Science 35 (2000) 1773–1785.
[17] X. Shui, D.D.L. Chung, Electrical resistivity of submicron-diameter carbon-filament compacts, Carbon 39 (2001) 1717–1722.
[18] M. Endo, H. Muramatsu, T. Hayashi, Y.A. Kim, M. Terrones, M.S. Dresselhaus, 'Buckypaper' from coaxial nanotubes, Nature 433 (2005) 476.
[19] D.A. Dikin, S. Stankovich, E.J. Zimney, R.D. Piner, G.H.B. Dommett, G. Evmenenko, Preparation and characterization of graphene oxide paper, Nature 448 (2007) 457–460.
[20] R. Holm, Electric Contacts: Theory and Applications, 4th ed. Springer-Verlag, Berlin, 1967.
[21] M. Braunovic, V. Konchits, N. Myshkin, Electrical Contacts: Fundamentals, Application and Technology, CRC Press, 2007.
[22] M.J. McAllister, J.L. Li, D.H. Adamson, H.C. Schniepp, A.A. Abdala, J. Liu, et al., Single sheet functionalized graphene by oxidation and thermal expansion of graphite, Chemistry of Materials 19 (2007) 4396–4404.
[23] P.C. Hiemenz, R. Rajagopalan, Principles of Colloid and Surface Chemistry, 3rd ed. Marcel Dekker, New York, 1997.
[24] N. Grossiord, J. Loos, O. Regev, C. Koning, Toolbox for dispersing carbon nanotubes into polymers to get conductive composites, Chemistry of Materials 18 (2006) 1089–1099.
[25] M.A.C.G. van de Graaf, J.H.H. ter Maat, A.J. Burggraaf, Microstructural development during pressing and sintering of ultra fine zirconia powders, Ceramic Powder, Elsevier, 1983, pp. 783–793.
[26] A.R. Cooper, L.E. Eaton, Compaction behavior of several ceramic powders, Journal of the American Ceramic Society 45 (1962) 97–101.
[27] R.L. Powell, G.E. Childs, American Institute of Physics Handbook, 3rd ed. McGraw-Hill, New York, 1972.
[28] K. Kendall, Electrical conductivity of ceramic powders and pigments, Powder Tech., 62, Elsevier, 1990, pp. 147–154.
[29] K. Kendall, NMcN Alford, J.D. Birchall, Elasticity of particles assemblies as measure of the surface energy of solids, Proceedings of the Royal Society of London. Series A 412 (1987) 269–283.
[30] B.J. Briscoe, M.J. Adams, Tribology in Particulate Technology, Adam Hilger, Bristol, 1987.
[31] R. Holm, Electric Contacts, Springer, Verlag Berlin, 1967.